Hindawi
Advances in Meteorology
Volume 2020, Article ID 4232138, 16 pages
https://doi.org/10.1155/2020/4232138

Research Article

Canopy Resistance and Estimation of Evapotranspiration above a Humid Cypress Forest

Bau-Show Lin,[1] **Huimin Lei**,[2] **Ming-Che Hu**,[3] **Supattra Visessri**,[4] **and Cheng-I Hsieh**[3]

[1]*Department of Horticulture and Landscape Architecture, National Taiwan University, Taipei 10617, Taiwan*
[2]*Department of Hydraulic Engineering, Tsinghua University, Beijing 100084, China*
[3]*Department of Bioenvironmental Systems Engineering, National Taiwan University, Taipei 10617, Taiwan*
[4]*Department of Water Resources Engineering, Chulalongkorn University, Bangkok 10330, Thailand*

Correspondence should be addressed to Cheng-I Hsieh; hsieh@ntu.edu.tw

Received 30 April 2019; Revised 18 September 2019; Accepted 8 October 2019; Published 4 January 2020

Academic Editor: Alessia Di Gilio

This study presented a two-year data set of sensible heat and water vapor fluxes above a humid subtropical montane Cypress forest, located at 1650 m a.s.l. in northeastern Taiwan. The focuses of this study were to investigate (1) the diurnal and seasonal variations of canopy resistance and fluxes of sensible heat and water vapor above this forest; and (2) the mechanism of why a fixed canopy resistance could work when implementing the Penman–Monteith equation for diurnal hourly evapotranspiration estimation. Our results showed distinct seasonal variations in canopy resistance and water vapor flux, but on the contrary, the sensible heat flux did not change as much as the water vapor flux did with seasons. The seasonal variation patterns of the canopy resistance and water vapor flux were highly coupled with the meteorological factors. Also, the results demonstrated that a constant (fixed) canopy resistance was good enough for estimating the diurnal variation of evapotranspiration using Penman–Monteith equation. We observed a canopy resistance around 190 (s/m) for both the two warm seasons; and canopy resistances were around 670 and 320 (s/m) for the two cool seasons, respectively. In addition, our analytical analyses demonstrated that when the average canopy resistance is higher than 200 (s/m), the Penman–Monteith equation is less sensitive to the change of canopy resistance; hence, a fixed canopy resistance is suitable for the diurnal hourly evapotranspiration estimation. However, this is not the case when the average canopy resistance is less than 100 (s/m), and variable canopy resistances are needed. These two constraints (200 and 100) were obtained based on purely analytical analyses under a moderate meteorological condition ($R_n = 600\ \mathrm{W{\cdot}m^{-2}}$, RH = 60%, $T_a = 20^{\circ}\mathrm{C}$, $U = 2\ \mathrm{m{\cdot}s^{-1}}$) and a measurement height around two times of the canopy height.

1. Introduction

Evapotranspiration (ET) and sensible heat have significant impacts on regional and global meteorology. In order to better understand heat, water vapor, and carbon dioxide fluxes between the vegetation and atmosphere, numerous measurements have been conducted on various terrestrial land surfaces (e.g., FLUXNET; see [1]). Based on these monitoring results, researchers have found that there is visible variability in heat, water vapor, and CO_2 fluxes between the seasons and sometimes between years. Sensible and latent heat fluxes were large in summer and relatively low during winter, and CO_2 assimilations were stronger in summer than in winter. However, the seasonal variations in sensible heat fluxes were stronger compared with both latent heat and CO_2 fluxes [2–4]. Therefore, the surface energy partitioning and the ratio of sensible heat flux (H) to latent heat flux (LE) also varied with seasons.

Because ET is a key process in the water cycle and in the surface energy budget, attention was paid to ET quantification methods (e.g., see review by [5]). The Penman–Monteith (P–M) equation, a method based on energy conservation and aerodynamic and surface (or canopy) resistances, is recommended worldwide [6] because of its standardization and universality in reference potential evapotranspiration estimation [7]. However, the difficulty in implementing P–M equation comes from parameterizing the resistance inputs, particularly the canopy (stomatal)

resistance [8–10], which controls water vapor passing in and out of the plant. High priced instruments (e.g., the photosynthesis systems) can be used to directly measure the canopy resistance; however, indirect parameterizing of this resistance is adopted more widely. Thus, models that deal with parameterizing the canopy resistance from meteorological data (i.e., net radiation, air temperature, wind speed, humidity, and soil water content) were proposed by many researchers [11–15].

Katerji and Rana [16] investigated the ET of six irrigated crops under the Mediterranean climate. Their results showed that adopting variable canopy resistance (calculated from meteorological data) to estimate evapotranspiration by the P–M equation has a significant advantage over constant (fixed) canopy resistance. Perez et al. [17] compared different methods for estimating canopy resistance under semiarid conditions in river valley with uniform grass. They showed that the constant canopy resistance (=70 s/m) might underestimate/overestimate evapotranspiration during summer/winter. Pauwels and Samson [18] pointed out that using the monthly averaged surface (canopy) resistance would lead to a better estimation of evapotranspiration at a seasonal time scale.

Above two semiarid grass sites, Lecina et al. [19] found that a fixed canopy resistance (70 s/m) could result in a good estimation of the daily reference evapotranspiration; but for the estimation of hourly reference evapotranspiration, variable canopy resistance values were needed. Kosugi et al. [20] reported a constant canopy resistance of 149 (s/m) for a temperate Japanese Cypress forest. Also, Hsieh et al. [21] used a constant canopy resistance for a year round estimation of hourly ET from grassland and found good agreement with the measurements. In short, a fixed constant canopy resistance may work for estimating ET rather than using variable canopy resistance, but the mechanism of why this works is still unsolved.

Among Earth surfaces, forests are one of the important ecosystems that affect our water resources and climate. Forests return large portions of precipitation water to the atmosphere through evapotranspiration, which greatly affect the hydrological cycle and relate to carbon fixation [22–24]. Montane cloud forests are one of the world's most endangered ecosystems because of their sensitivity to changes in unique ecological conditions [25, 26]. Understanding ET from montane cloud forests continues to be an active research topic [27, 28]. In Taiwan, the Chamaecyparis (Cypress) forest grows across the whole island, varying in species composition and habitat conditions [29]. This study investigated the ET of a humid montane Cypress forest with a relatively homogeneous slope topography in northern Taiwan from a two-year eddy-covariance measurement data set. The purposes of this research are to (1) reveal the diurnal and seasonal variations and patterns of canopy resistance, sensible heat flux, and evapotranspiration above a mountain forest, (2) investigate the mechanism of why a constant (fixed) canopy resistance may work when implementing Penman–Monteith equation for ET estimation, (3) examine the performance of Penman–Monteith equation on estimating evapotranspiration in different seasons, (4) investigate the relationship between net radiation, sensible heat, and latent heat fluxes, and their influences on meteorological conditions above the forest.

2. Experiment

2.1. Site Description and Experimental Setup. Meteorological and surface flux measurements were made from May 1, 2005, to April 30, 2007, above a homogeneous Cypress forest at 1,650 m a.s.l. in northeastern Taiwan (24°35′27.4″N, 121°29′56.3″E). The site is at Chi-Lan Mountain and close to the Yuan Yang Lake ecosystem, which is declared a nature preserve in order to protect it against anthropogenic disturbances. The topography of this site is a relatively homogeneous slope of 14 degrees facing the southeastern direction and extending for 2 km and the Cypress forest covers an altitude range from 1,650 to 2,432 m a.s.l. Frequently covered by fog and cloud, the site received relatively less solar radiation and featured a temperate heavy moist climate. From previous record, the average annual air temperature was 13°C, and annual precipitation was around 4,000 mm. In this Cypress forest, *Chamaecyparis obtusa* var. *formosana* and *Chamaecyparis formosensis* are the predominant species; the understory is mainly comprised by *Rhododendron formosanum* [30]. Due to frequent precipitation, the soil water content at 30 cm was about 0.3–0.4 (m^3/m^3) and relatively steady annually [27]. Soil water status has no or minor influence on the daily ET and, thus, plays an unimportant role in regulating the water use of this Cypress forest [27]. Previous studies at Chi-Lan Mountain cloud forest in Taiwan indicated that the endemic tree species—yellow Cypress (Chamaecyparis obtusa var. formosana)—is well adapted to conditions of moist atmosphere and lower incident radiation [31–33]. The ecosystem CO_2 uptake was found to be only marginally reduced, and small evapotranspiration still occurred during the fog periods [33, 34]. At this site, the canopy was closed and uniform with a leaf area index (LAI) of 6.3 m^2/m^2 [35], and hence the soil heat flux was small all year round. More details about the site can be found in the work by Chang et al. [35] and Chu et al. [27].

The eddy-covariance method was applied to determine surface fluxes over this subtropical evergreen coniferous forest. The monitoring instruments were attached to a 23.4 m height walkup tower, where the average canopy height was 10.3 m. Around the tower site, the plantation exhibits a relatively narrow age range; trees were planted between 1961 and 1978 [30]. The tower was located in the north-westerly end of the plantation. The terrain around the tower site was relatively flat.

The net radiation was measured with a CNR1 radiometer (Kipp & Zonen, Delft, The Netherlands), which separates the upward and downward short wave and long wave radiation components. The air temperature and humidity were measured with a HMP45A sensor (Vaisala, Helsinki, Finland). The radiometer and temperature/humidity sensors were installed at 22.5 and 23.5 m above the ground, respectively. Net radiation (R_n), air temperature (T_a) and relative humidity (RH) were all recorded on a data

logger and averaged for a 30 min period. The eddy-covariance system was installed at 24 m above the ground. The three-dimensional wind velocity and virtual potential temperature were measured with an ultrasonic anemometer (R. M. Young 81000, Traverse City, Michigan, USA). The water vapor concentration was measured with a LI-7500 open path infrared gas analyzer (LI-COR, Lincoln, Nebraska, USA). Wind velocity, water vapor concentration, and virtual potential temperature were collected on a portable laptop at 10 Hz and the averaging period was half an hour. All instruments were powered by a series of 12 VDC batteries.

2.2. Data Processing. For the flux calculation, the general FLUXNET standard process (e.g., [36, 37]) including detrending, despiking, and spectral correction were applied. Detrending was done by removing the linear trend of the raw data. Spikes outside the ±3 standard deviation were replaced with the interpolated values. If the number of spikes exceeded 1% of the total number of each measurement run, then this run was abandoned. The spectral correction (frequency filtering) was done following Moore [38]. Time lags between measured scalars and vertical velocity were removed, and the planar fit method was applied to rotate the three velocity components into the mean streamline coordinate system [39]. The Webb–Pearman–Leuning correction was applied to correct the fluctuation of air density [40]. The data was collected during the period from May 2005 to April 2007.

The 30 min data were then divided into two seasons: warm (May to October) and cool seasons (November to April). Missing data (due to weather conditions, instruments maintenance, etc.,) were excluded from the analysis. The data available rates for the warm and cool seasons of 2005 and 2006 were 34.42, 36.03, 47.78, and 70.11%, respectively (also listed in Table 1). In each season, data were averaged to get a seasonal mean of diurnal variation. Due to instruments maintenance and weather condition, the data of March, 2006, was discarded. The average air temperature, relative humidity, wind speed, and vapor pressure deficit diurnal variations for the period of May 2015–April 2017 are shown in Figures 1(a)–1(d). The time zone of this site is UTC + 8 hours. In warm seasons, the temperature varied between 18 and 20°C and in cool seasons it ranged between 11 and 14°C (Figure 1(a)). For both warm and cool seasons, the humidity patterns were different from our normal experience in this foggy montane forest site. The humidity remained roughly constant (around 85–93%) from 00:00 to 06:00, then increased linearly to around 100% from 07:00 to 16:00 (fog started forming around 15:00), and then dropped linearly to around 90% from 17:00 to 24:00 (Figure 1(b)). For the wind field, the obvious valley-mountain wind diurnal cycles for all seasons were noticed, as shown in Figure 1(c), and the wind speed ranged between 1 and 2 (m/s). As to the vapor pressure deficit diurnal patterns (Figure 1(d)), they were inversely related to the patterns of relative humidity. Also, the precipitation in 2005 warm and cool seasons and 2006 warm and cool seasons were 4061, 1232, 2760, and 1086 mm, respectively (Figure 1(e)). At this site, the typhoon period is within the warm season; hence the warm seasons generally have higher precipitation than the cool seasons.

3. Methods

In this section, the Penman–Monteith equation (used for estimating ET) was first described and the role of canopy resistance was then discussed.

3.1. Penman–Monteith Equation. The Penman–Monteith equation for calculating latent heat flux, LE ($W \cdot m^{-2}$), can be expressed as follows [6]:

$$\mathrm{LE} = \frac{\Delta Q_n}{\Delta + \gamma\left(1 + r_c/r_a\right)} + \frac{\rho c_p D/r_a}{\Delta + \gamma\left(1 + r_c/r_a\right)}, \quad (1)$$

where Δ is the slope of the saturation vapor pressure-temperature curve calculated at the air temperature T_a, γ ($=Pc_p/0.622L_v$) is the psychrometric constant, P is the air pressure, ρ ($\approx 1.2\,kg \cdot m^{-3}$) is the mean air density, c_p ($=1005\,J \cdot kg^{-1} \cdot K^{-1}$) is the specific heat for air, L_v ($=2.46 \times 10^6\,J \cdot kg^{-1}$) is the latent heat of vaporization, Q_n ($=R_n - G$) is the available energy, G is the soil heat flux, D is the vapor pressure deficit, r_a is the aerodynamic resistance of water vapor ($s \cdot m^{-1}$), and r_c is the canopy resistance ($s \cdot m^{-1}$). The first term on the right hand side in (1) is generally called as the energy term ($\mathrm{LE}_{\_eq}$) and represents the contribution from available energy; and we can define a direct energy transfer coefficient (t_c)

$$t_c = \frac{\Delta}{\Delta + \gamma\left(1 + r_c/r_a\right)}, \quad (2)$$

which describes how much available energy (Q_n) would be transferred into LE directly. The second term on the right hand side is called the atmospheric demand term ($\mathrm{LE}_{\_vpd}$) and describes the ET demanding from the atmosphere. Now, equation (1) can be rewritten as

$$\mathrm{LE} = t_c * Q_n + \mathrm{LE}_{\_vpd}. \quad (3)$$

If a linear relationship exists between Q_n and LE, that is, $\mathrm{LE} = a * Q_n + b$. Then the regression slope a should be close to t_c, and $\mathrm{LE}_{\_vpd}$ is close to the intercept b and relatively constant. In (1), r_a can be calculated by

$$r_a = \frac{\left[\ln\left(z/z_o\right)\right]\left[\ln\left(z/z_{ov}\right)\right]}{k^2 U} = \frac{\ln\left(z/z_{ov}\right)}{k u_*}, \quad (4)$$

where k (=0.4) is the von Karman constant, u_* is the friction velocity ($m \cdot s^{-1}$), z is the measurement height, z_o is the surface roughness ($\cong 0.1h$, h is the average canopy height) for momentum, z_{ov} is the surface roughness ($\cong 0.01h$) for water vapor, and U is the mean wind speed at measurement height z.

When r_c approaches zero, then (1) becomes the Penman equation:

$$\mathrm{LE} = \frac{\Delta Q_n + \rho c_p D/r_a}{\Delta + \gamma}, \quad (5)$$

Table 1: Summary of energy partition for LE and H Bowen ratio, energy closure ratio, direct energy transfer coefficient, and data available rate.

Season	Energy partition LE	Energy partition H	Bowen ratio	Energy closure ratio	Averaged t_c	Data available rate (%)
2005 warm	0.35	0.50	1.28	0.85	0.35	34.42
2005 cool	0.11	0.63	4.20	0.74	0.12	36.03
2006 warm	0.31	0.53	1.39	0.84	0.32	47.78
2006 cool	0.20	0.56	2.15	0.76	0.20	70.11

t_c: direct energy transfer coefficient, defined in equation (1).

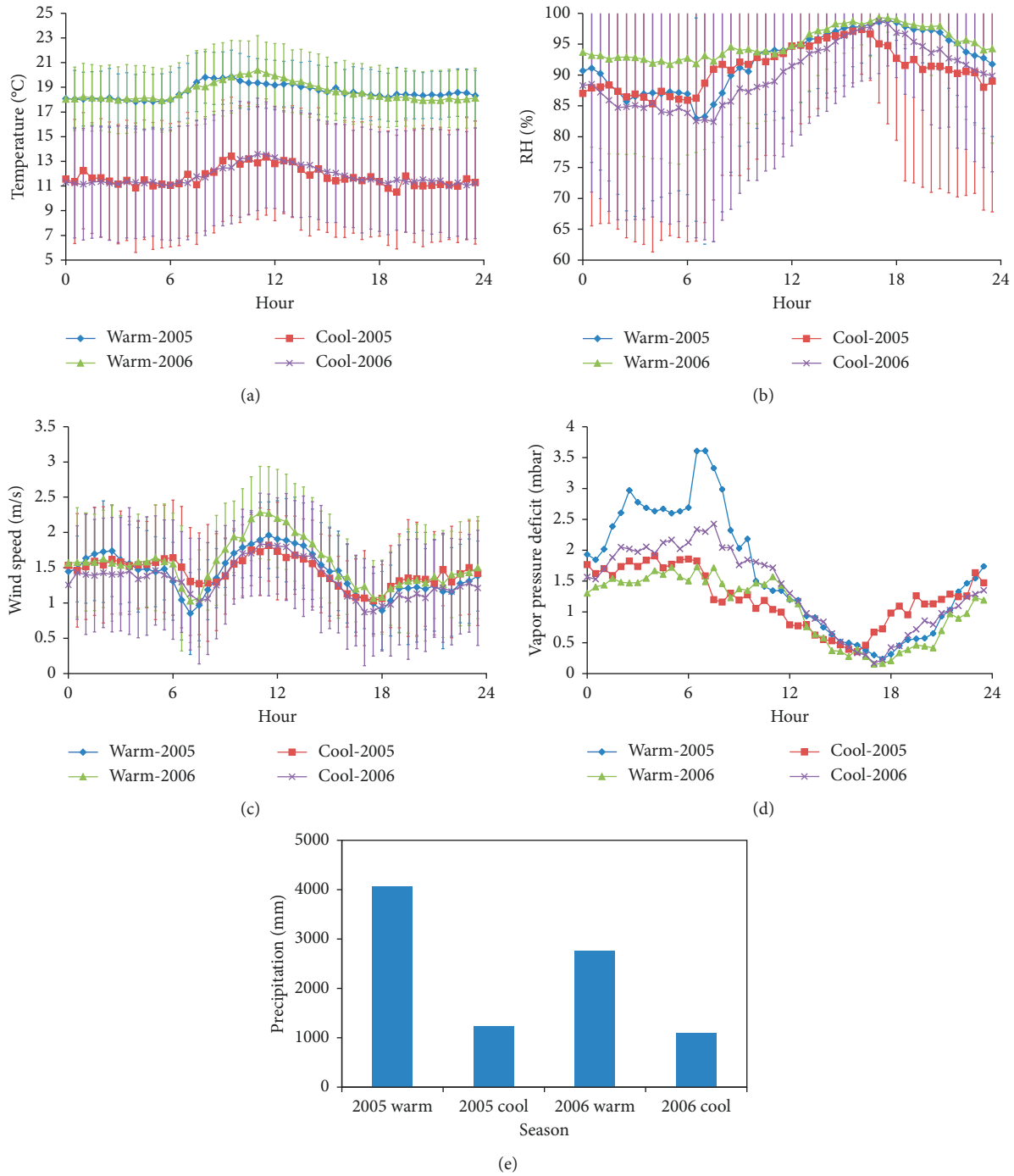

Figure 1: Averaged diurnal variations of (a) air temperature, (b) relative humidity, (c) wind speed, and (d) vapor pressure deficit for the warm (May to Oct.) and cool (Nov. to April) seasons of 2005–2006. The vertical bars indicate the standard deviations. (e) Precipitation for each season.

for calculating the potential evapotranspiration (PET). Also, when the vapor pressure deficit, D, approaches zero, (1) reduces to

$$\mathrm{LE} = \frac{\Delta Q_n}{\Delta + \gamma\left(1 + r_c/r_a\right)}. \tag{6}$$

Equation (6) is the so-called equilibrium evapotranspiration (LE_eq), and ET is mainly driven by the available energy under this condition.

Following McNaughton and Jarvis [41], (1) can also be expressed as

$$\mathrm{LE} = \Omega\frac{\Delta Q_n}{\Delta + \gamma} + (1 - \Omega)\frac{\rho C_p D}{\gamma r_c}, \tag{7}$$

where the decoupling coefficient Ω is defined as

$$\Omega = \frac{(\Delta/\gamma) + 1}{(\Delta/\gamma) + 1 + \left(r_c/r_a\right)} = \frac{(\Delta + \gamma)/\gamma}{(\Delta + \gamma)/\gamma + \left(r_c/r_a\right)}. \tag{8}$$

The decoupling coefficient indicates the relative importance of the energy term in (1). When r_c approaches 0, Ω becomes unity; this represents the daytime condition with a wet canopy surface where the role of r_c is ignored. When r_c approaches infinite, Ω becomes zero; this represents the night time condition in which the ET portion from the energy term (LE_eq) is zero. Jarvis and McNaughton [42] showed that forests generally have smaller decoupling coefficient than short grass and crops. This implies that forests are very closely coupled to the atmosphere above and that the evapotranspiration rate is thus dominated by the atmospheric demand term.

3.2. Sensitivity of P–M Equation on Canopy Resistance. As stated in the Introduction section, an interesting phenomenon in implementing P–M equation is that some research concluded that a fixed constant r_c is good enough (e.g., [19]) but some others suggested variable r_c (e.g., [12]) is needed. To investigate the sensitivity of LE estimation to a change of the canopy resistance, we consider the following:

$$\frac{\partial \mathrm{LE}}{\partial r_c} = -\frac{\gamma\left(\Delta Q_n + \rho C_p D/r_a\right)}{r_a\left(\Delta + \gamma\left(1 + \left(r_c/r_a\right)\right)\right)^2}. \tag{9}$$

Equation (9) represents the sensitivity of the P–M equation with respect to r_c and describes how LE estimation would be varied by a unit increase of r_c. Now substitute r_a with equation (4), we then have

$$\frac{\partial \mathrm{LE}}{\partial r_c} = -\frac{\gamma\left(\Delta Q_n + \left(\rho C_p D k^2 U/\left(\ln\left(z/z_0\right)\ln\left(z/z_{ov}\right)\right)\right)\right)}{\left(\left(\ln\left(z/z_0\right)\ln\left(z/z_{ov}\right)\right)/\left(k^2U\right)\right)\left(\Delta + \gamma\left(1 + r_c k^2 U/\left(\ln\left(z/z_0\right)\ln\left(z/z_{ov}\right)\right)\right)\right)^2}. \tag{10}$$

Equation (10) explicitly describes that the ratio of $\partial LE/\partial r_c$ is also a function of wind speed in addition to the other three meteorological parameters: net radiation, temperature, and vapor pressure deficit. Using equation (4) and setting the measurement height z as two times of the canopy height ($z = 2h$), one obtains $r_a = 99/U$, and equation (10) reduces to

$$\frac{\partial \mathrm{LE}}{\partial r_c} = -\frac{\gamma\left(\Delta Q_n + \left(\rho C_p D U/99\right)\right)}{(99/U)\left(\Delta + \gamma\left(1 + \left(r_c U/99\right)\right)\right)^2}. \tag{11}$$

Also, in this study, with the measured LE and rearranging equation (1), the measured r_c was calculated by the following:

$$r_c = \left(\frac{\Delta}{\gamma}\frac{Q_n - \mathrm{LE}}{\mathrm{LE}} - 1\right)r_a + \frac{\rho C_p}{\gamma}\frac{D}{\mathrm{LE}}. \tag{12}$$

4. Results and Discussion

In this section, we first present the temporal variation of R_n, H, LE, and G, the characteristics of ET, and energy partition for the warm and cool seasons of the year 2005-2006 at this humid montane forest. Then we discuss the performance of P–M equation, the role of canopy resistance, the decoupling coefficient, and the direct energy transfer rate.

4.1. Energy Partition. The averaged diurnal variations of G, R_n, H, and LE in warm and cool seasons during the year 2005-2006 are plotted in Figure 2. Since at this site the canopy was closed, the soil heat fluxes (G) for the warm and cool seasons were all very small (Figure 2(a)). In Figure 2(a), the maximum and minimum soil heat fluxes are 8 and −4 (W/m^2), respectively; and the soil heat flux measurements were not available in 2006 cool season due to the soil heat flux plate maintenance. For R_n, as expected, warm seasons received more net radiation than cool seasons did (Figure 2(b)); the maximum R_n for warm and cool seasons were around 514 and 437 (W·m^{-2}), respectively. For H, there was no major tendency between warm and cool seasons (Figure 2(c)); the maximum H varied between 257 and 311 (W·m^{-2}). As to LE, in both warm seasons the LE peak value could be as large as 175 W·m^{-2}, but the peak values were only 50 and 100 (W·m^{-2}) for 2005 and 2006 cool seasons, respectively (Figure 2(d)). Why the 2006 cool season had a higher LE than the 2005 cool season? This was because the relative humidity was lower during day time in 2006 cool season (Figure 1(b)) and resulted in a lower canopy resistance [12, 43]. This relatively low RH also created a relatively higher atmospheric demand for ET in the cool season of the year 2006. It was noticed that, as shown in Figure 2(b), the cool season 2005 received less R_n than the warm season 2005, but the cool season 2005 had a higher H than the warm season 2005 had. This was due to the low LE in the cool season of 2005 and the major portion of R_n was distributed into H. This revealed that the meteorological condition was coupled with the biological

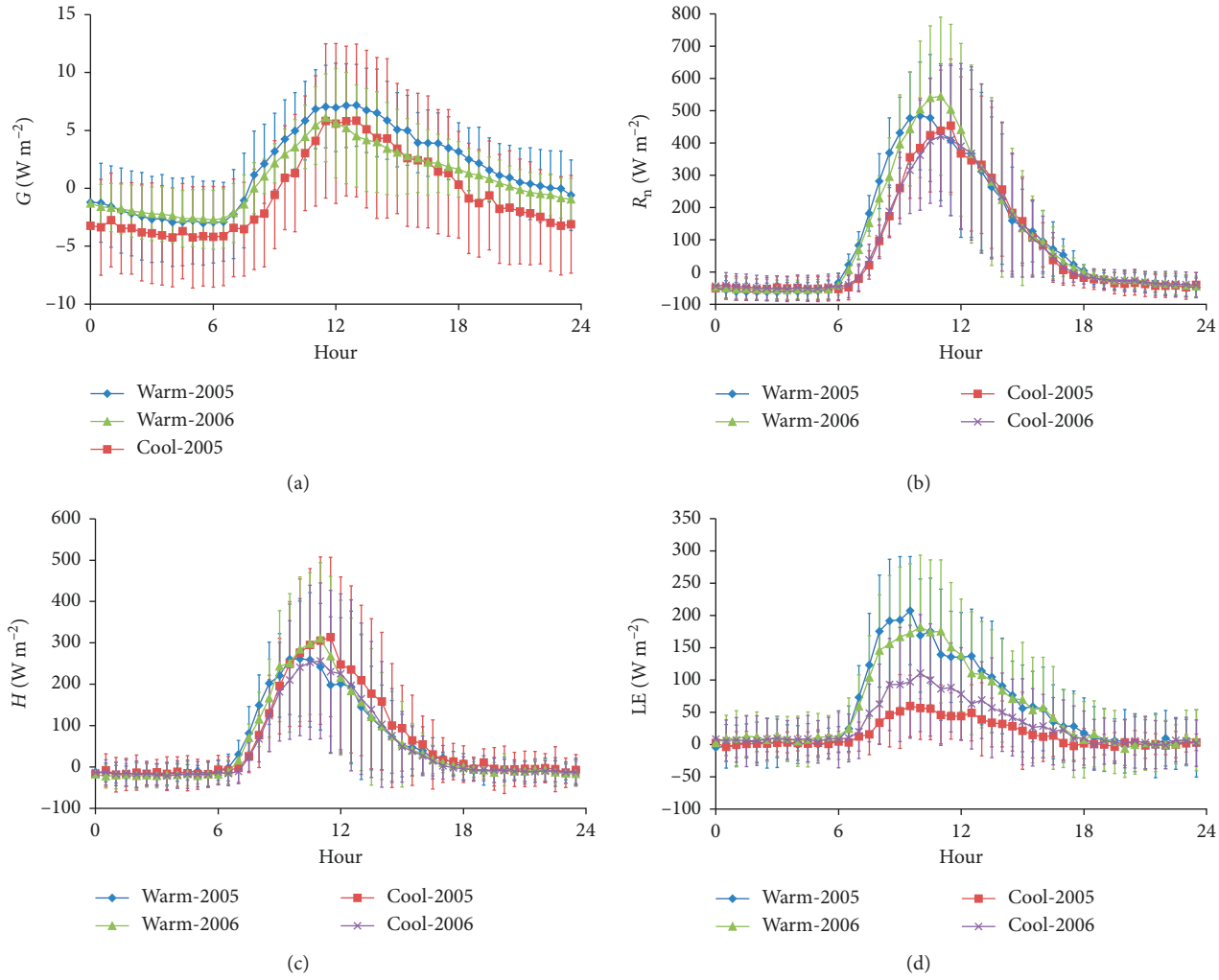

Figure 2: Averaged diurnal variations of (a) G, (b) R_n, (c) H, and (d) LE for the warm (May to Oct.) and cool (Nov. to April) seasons of 2005–2006. The vertical bars indicate the standard deviations.

condition (i.e., r_c). In other words, low air temperature and high relative humidity caused a higher canopy resistance and then resulted in a lower LE and then produced a higher sensible heat, which would later on warm the air more. This also demonstrated how vegetation could change the micrometeorology.

To check the energy partition of this site, the scatter plots of H v.s. R_n and LE v.s. R_n for each season are shown in Figure 3. In the warm seasons of 2005 and 2006, half of the R_n was transferred into H and around 35% of R_n was transferred into LE. For cool season 2005, only $0.11R_n$ was transferred into LE and $0.63R_n$ was distributed into H. As for the cool season of 2006, LE was about $0.2R_n$ and H was around $0.56R_n$. In short, Figure 3 shows that in cool seasons, ET was smaller and resulted in a higher percentage of R_n distributing into H. Figures 2 and 3 indicate that the ET phenomenon controlled the micrometeorology on this site. Also, from Figures 2 and 3, there is a hysteresis between R_n and ET. Both biotic factors (e.g., canopy resistance, root water potential) and abiotic factors (e.g., soil water status, boundary layer processes) contribute to the LE hysteresis [44]. In our site, due to frequent precipitation, the soil water content at 30 cm was about 0.3–0.4 (m^3/m^3) and relatively steady annually; so soil water status has no or minor influence on the daily ET. Hence, the hysteresis of LE in this site is attributed to the canopy resistance and boundary layer process.

These energy partition results, Bowen ratios (H/LE), and energy closure ratio for these four seasons were also summarized in Table 1. For warm seasons, the energy closure was about 85%; for cool seasons, it was around 75%. These energy closure ratios are normal compared with the literature.

4.2. Estimation of Latent Heat Flux. For estimating LE, we adopted Penman–Monteith equation (equation 1) in conjunction with a constant canopy resistance. The comparisons between the seasonal averages of half-hourly measured and predicted LE for each season are shown in Figure 4. The regression analyses for Figure 4 are also summarized in Table 2. In Figure 4, the fixed constant canopy resistance adopted in each season was the average canopy resistance

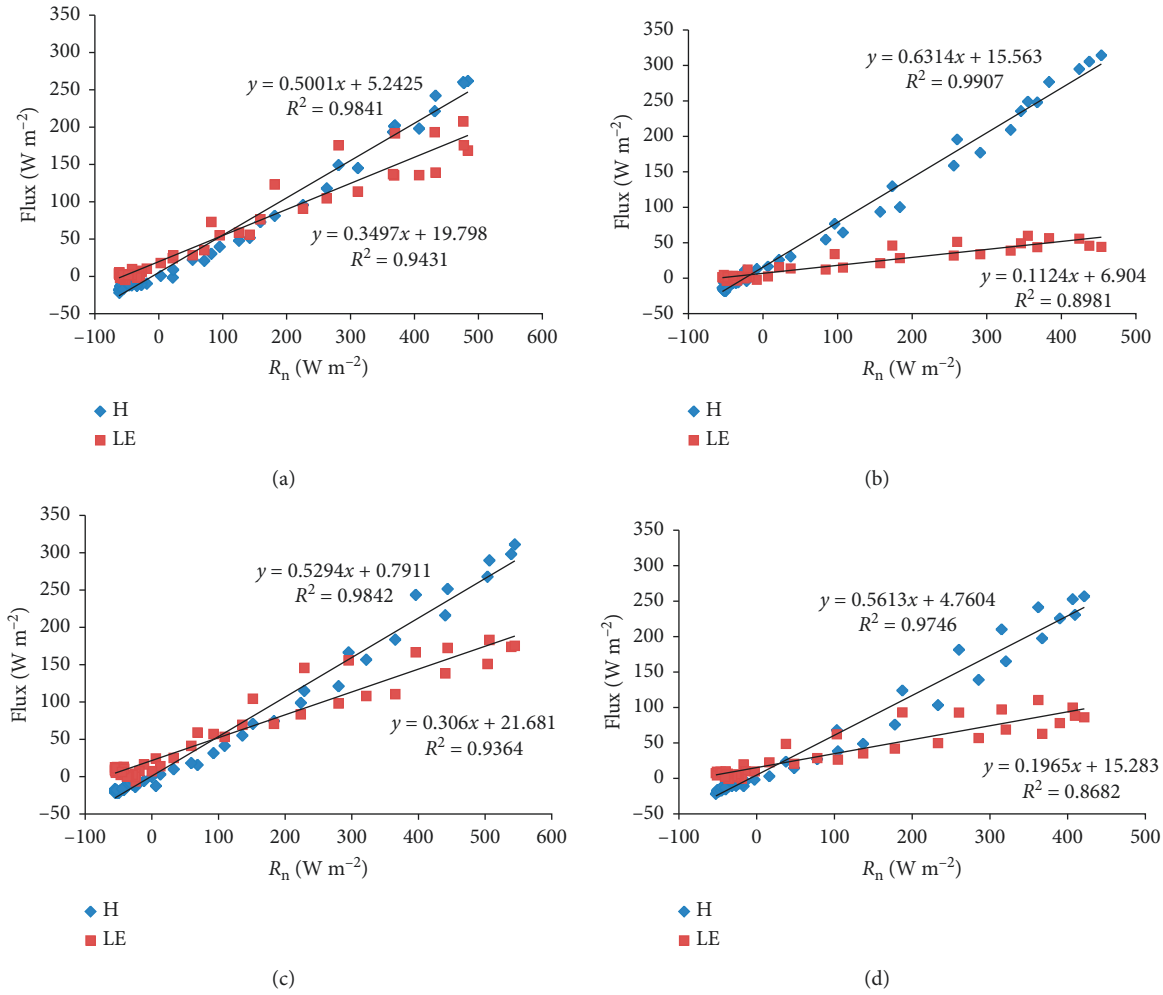

FIGURE 3: Scatter plots of H and LE as a function of R_n for the season of (a) warm 2005, (b) cool 2005, (c) warm 2006, and (d) cool 2006. H LE and R_n are in (W·m^{-2}).

between 10:00 and 14:00 (the period when the canopy surface was dry). The canopy resistance values were calculated by equation (12) with the measured LE and R_n. The average and maximum canopy resistances for each season were also listed in Table 2. For complete purpose, we also provided the comparisons between all the half-hourly (not averaged) measured and predicted LE for each season in the Appendix.

From Figure 4 and Table 2, it is clear that P–M method could predict LE well (R^2 ranged from 0.91–0.98) with a fixed constant r_c. The average canopy resistances for warm and cool seasons of 2005 and 2006 were 185, 673, 201, and 320 (s/m), respectively. It is noticed that the average canopy resistances for warm seasons were around 190 (s/m), but the average canopy resistances for cool seasons were much higher (more than 320). This difference of canopy resistance between the warm and cool seasons was attributed to the air temperature (Figure 1(a)), since low temperature resulted in high canopy resistance [12].

To further examine the variation of r_c during day time (07:00–17:00), we plotted the diurnal course of r_c in Figure 5. Notice that no matter in warm or cool season, r_c had its lowest value around 07:00 in the morning and then increased linearly to its highest value around 12:00 then remained constant till around 1500 and then dropped. This diurnal variation of r_c could be explained by the following: in the early morning ET occurred under wet surface condition (fog water remained on the leaf surface), so r_c was small (and this should close to PET, shown in Figure 6); then r_c was increased due to a drier canopy surface, and around 15:00 the fog started forming and caused a wet canopy surface and resulted in a reduction of r_c. It is noticed that this drop of r_c would not happen for a forest (or other vegetation) with dry canopy surface in the late afternoon (e.g., [45, 46]).

Using equation (5), we presented the calculated PET and measured LE in Figure 6 for each season. Figure 6 shows that in the early morning (06:00–07:00) and late afternoon (17:00–18:00) the ET was close to PET for all the seasons. This again confirms that in the early morning and late afternoon, the canopy surface was wet and created a relatively high ET. Also, recalling from the P–M equation, there are two sources for LE, one is the energy term (LE_eq) and the other is the atmospheric demand term (LE_vpd). To quantify the relative magnitude of these two terms, Figure 7 shows the diurnal

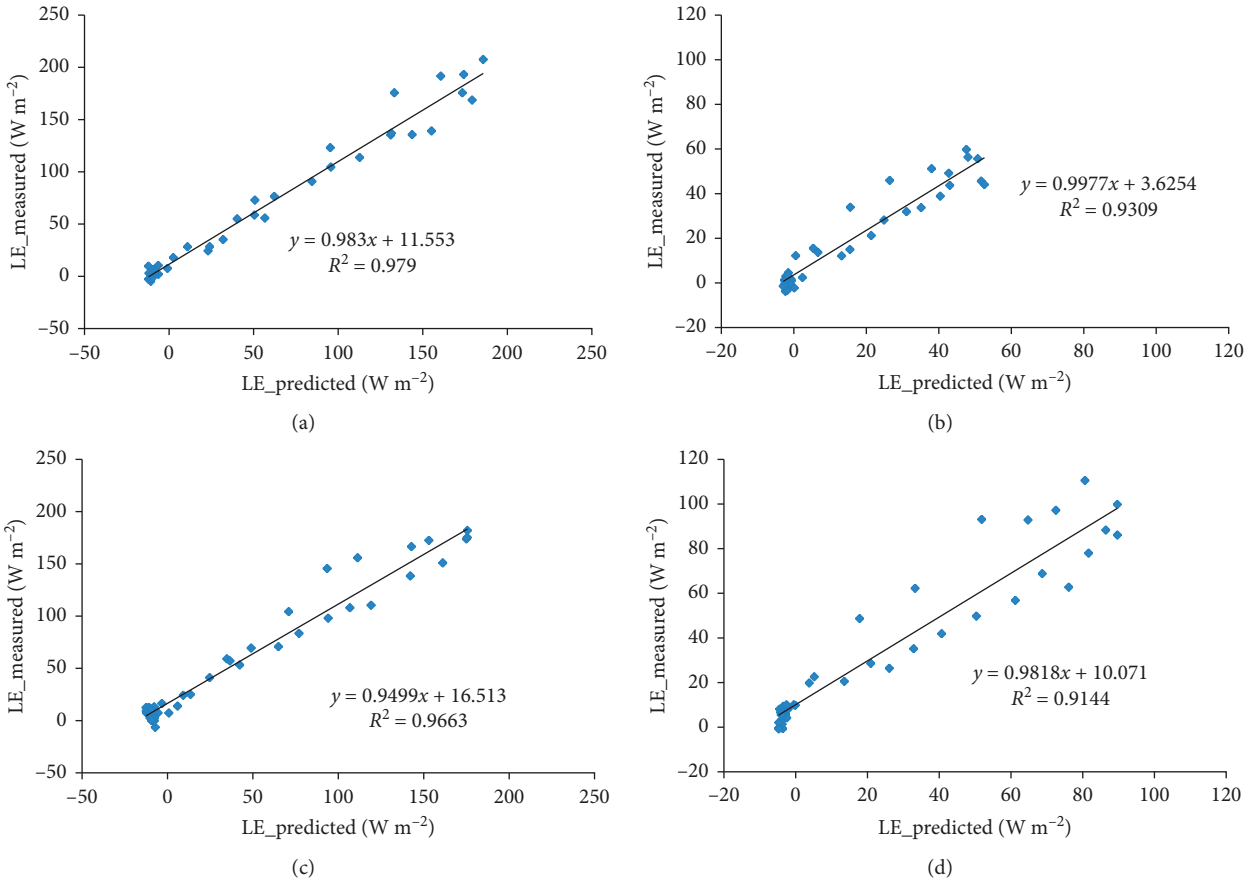

Figure 4: Comparisons between measured and predicted LE (W·m^{-2}) for the season of (a) warm 2005, (b) cool 2005, (c) warm 2006, and (d) cool 2006.

Table 2: Summary of regression analysis between measured and predicted LE (W·m^{-2}). $Y = aX + b$; Y is measured LE; X is predicted LE.

Season	a	b (W·m^{-2})	R^2	Average r_c (s/m)	Maximum r_c (s/m)
2005 warm	0.98	11.55	0.98	185	226
2005 cool	1.00	3.63	0.93	673	831
2006 warm	0.95	16.51	0.97	201	229
2006 cool	0.98	10.07	0.91	320	418

variation of these two terms as well as measured and predicted LE. It is obvious that the energy term was much bigger than the LE$_{_vpd}$ term. The LE$_{_vpd}$ term was very small at this humid montane forest.

4.3. The Role of Canopy Resistance. From Figures 4 and 5 and Table 2, it is noticed that though r_c varied with time, a constant r_c could still provide good estimations of LE for the whole diurnal period. To explore the sensitivity of the P–M equation estimated LE to r_c, we considered equation (11), which describes how much of the estimated LE is increased with a unit increase of r_c. Equation (11) reveals that the ratio of $\partial LE/\partial r_c$ is a function of r_c and four meteorological parameters: U, R_n, T_a, and RH. To explicitly determine the variation of $\partial LE/\partial r_c$ with respect to r_c under different meteorological conditions, the following steps were taken. Firstly, a moderate meteorological condition was selected as the baseline, where $R_n = 600$ (W/m^2), $U = 2$ (m/s), RH = 0.6, and $T_a = 20$ (°C). Secondly, we varied one of the four meteorological parameters (i.e., R_n, T_a, U, or RH) each time, and the other three parameters remained constant as the baseline values.

Now, given the baseline condition: $U = 2$ m/s, RH = 0.6, and $T_a = 20$°C, we plotted the variations of $\partial LE/\partial r_c$ with respect to r_c for R_n from 50 to 800 (W/m^2) in Figure 8(a). From Figure 8(a), we noticed that (1) when r_c is large (say greater than 500 s/m), $\partial LE/\partial r_c$ is small (<−0.2) irrelevant to the magnitude of R_n; (2) when $r_c = 200$ (s/m), a unit increase of r_c would cause only 0.2 to 0.8 unit decrease on LE estimation; (3) however, if $r_c = 100$ (s/m), then $\partial LE/\partial r_c$ could reach 1.4 when R_n is 600 (W·m^{-2}); and (4) when R_n is smaller, $\partial LE/\partial r_c$ is smaller for the same r_c. Figure 8(b) is the same as Figure 8(a), but for different wind speeds (U ranged from 0.05 to 6 m/s with $R_n = 600$ W·m^{-2}, RH = 0.6, and $T_a = 20$°C). Figure 8(b) has the similar pattern as in Figure 8(a) and shows that (1) if U is small (≤0.05 m/s), then the ratio of $\partial LE/\partial r_c$ is around −0.08 and does not change

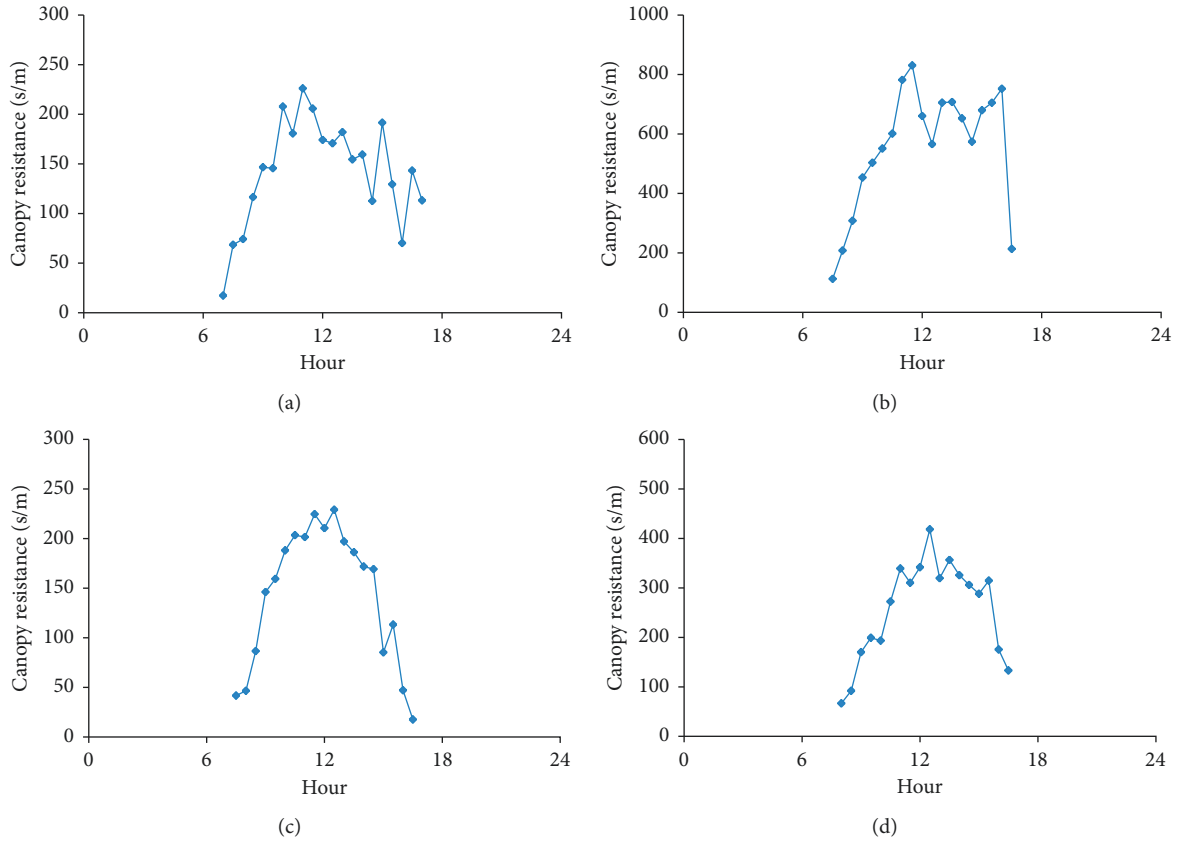

Figure 5: Diurnal variations of canopy resistance (s/m) for the season of (a) warm 2005, (b) cool 2005, (c) warm 2006, and (d) cool 2006.

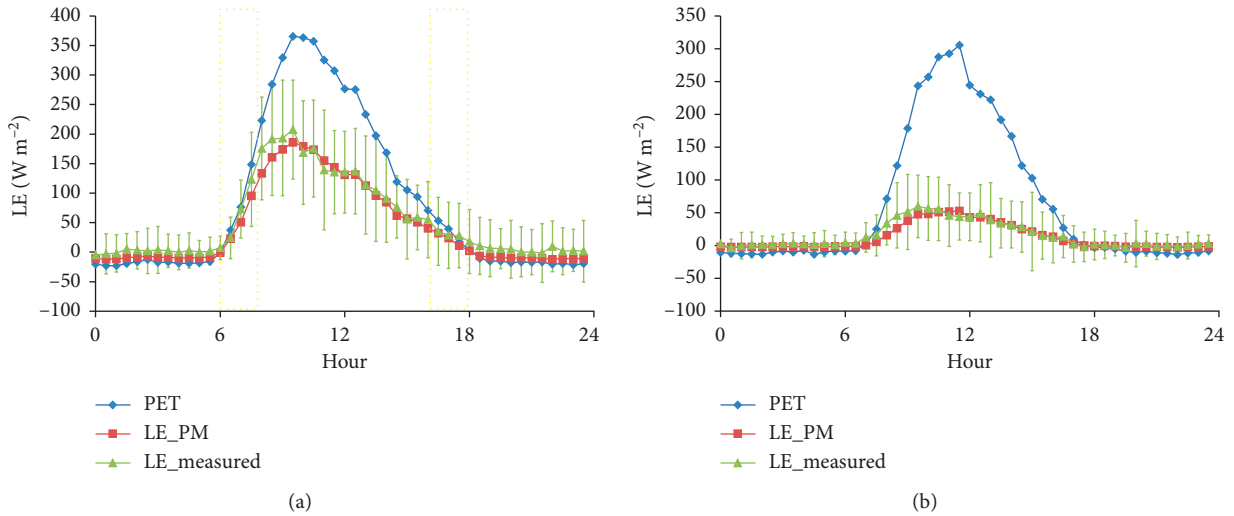

Figure 6: Continued.

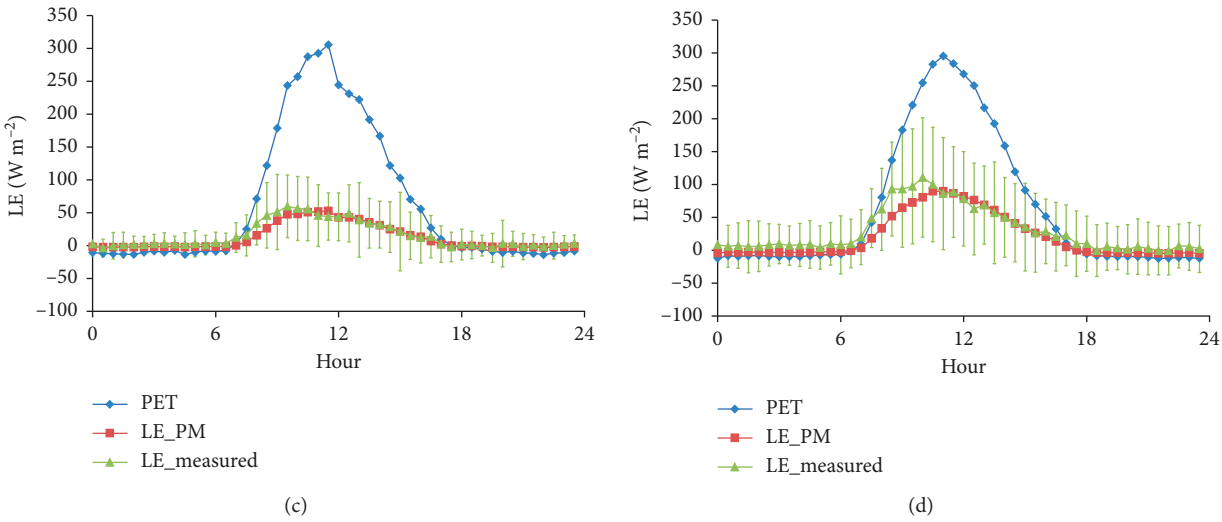

Figure 6: Comparisons between potential evapotranspiration (PET), predicted LE by PM equation (LE_PM), and measured LE (LE_measured) for the season of (a) warm 2005, (b) cool 2005, (c) warm 2006, and (d) cool 2006. The yellow box highlights the region where LE_measured is close to PET. The vertical bars indicate the standard deviations.

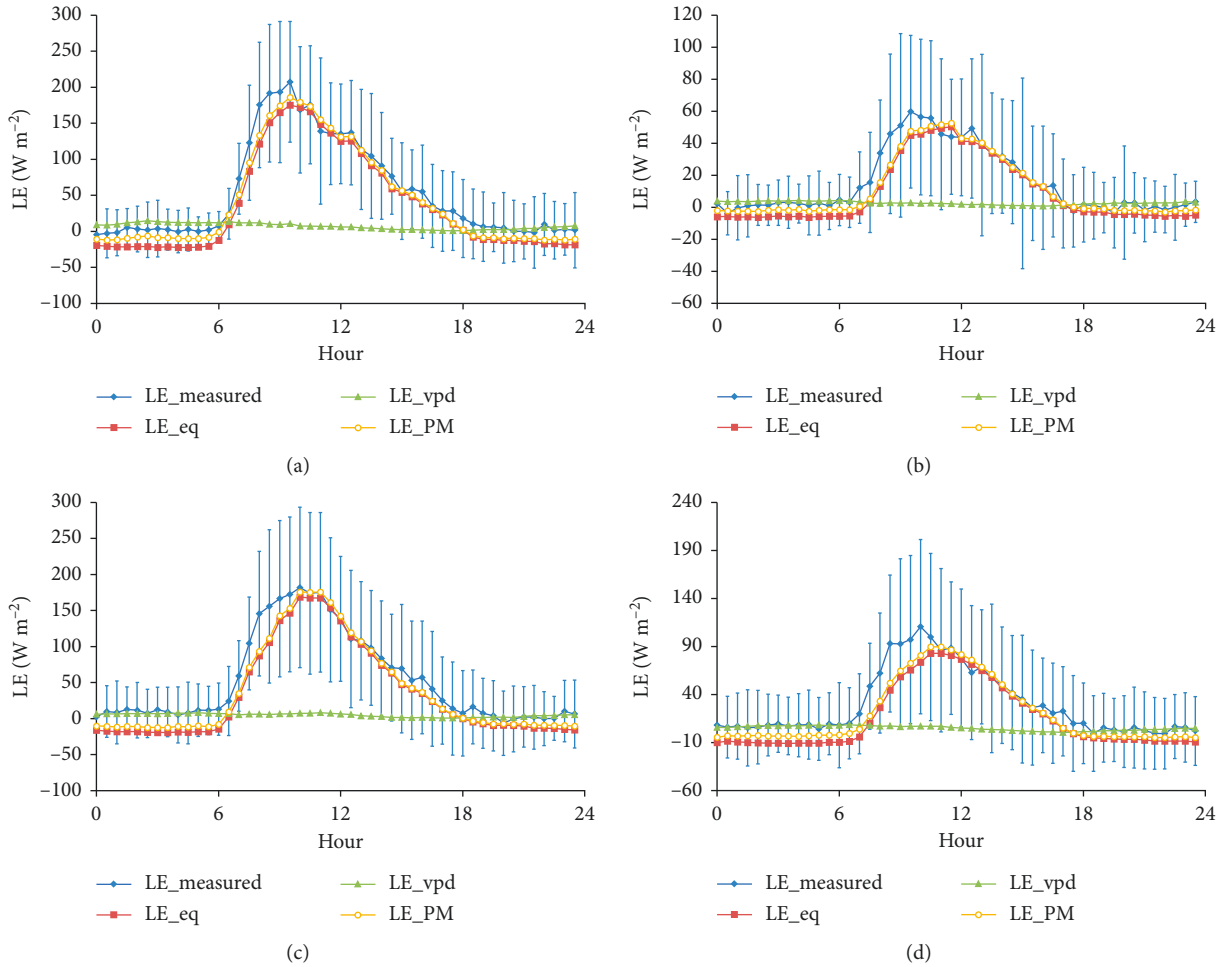

Figure 7: Diurnal variations of measured LE (LE_measured), LE predictions by PM equation (LE_PM), LE at equilibrium (LE_eq), and the LE contribution by vpd (LE$_{_vpd}$) for the season of (a) warm 2005, (b) cool 2005, (c) warm 2006, and (d) cool 2006. The vertical bars indicate the standard deviations.

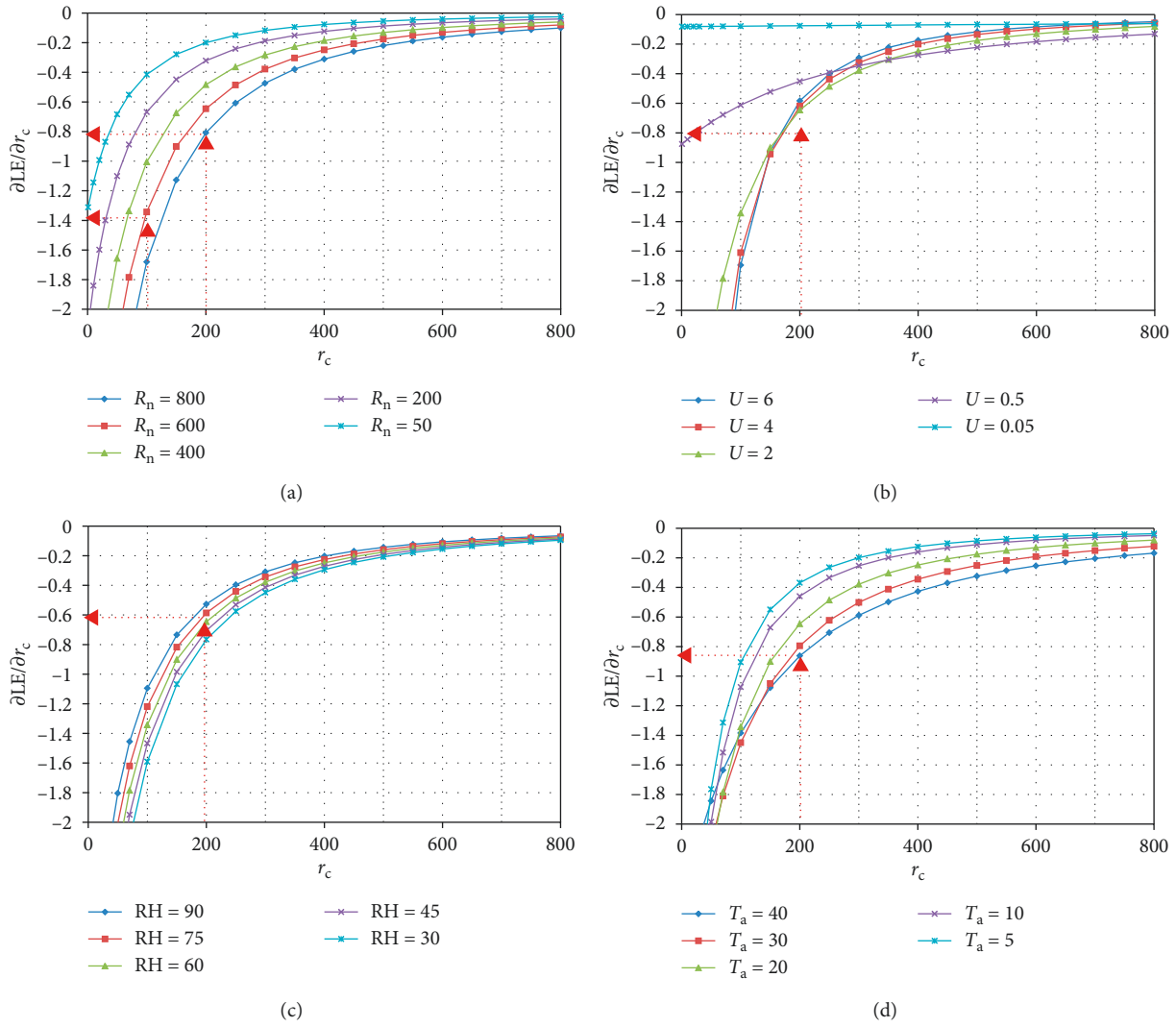

Figure 8: $\partial LE/\partial r_c$ as a function of r_c (m/s) under different meteorological conditions (a) $U = 2$ (m/s), $T_a = 20$ (°C), RH = 60%; (b) $R_n = 600$ (W·m^{-2}), $T_a = 20$ (°C), RH = 60%, (c) $R_n = 600$ (W·m^{-2}), $U = 2$ (m/s), $T_a = 20$ (°C), and (d) $R_n = 600$ (W·m^{-2}), $U = 2$ (m/s), RH = 60%.

Table 3: Values of $\partial LE/\partial r_c$ with different r_c under $R_n = 600$ (W/m^2), RH = 0.6, $U = 2$ (m/s) at two different temperatures [$T_a = 20$ and 10 (°C)].

r_c (s/m)	$\partial LE/\partial r_c$ [$T_a = 20$ (°C)]	$\partial LE/\partial r_c$ [$T_a = 10$ (°C)]
70	−1.78	−1.52
100	−1.34	−1.07
200	−0.65	−0.46
400	−0.25	−0.16

with r_c much; (2) for the cases where U is larger than 2 (m/s), the curves of $\partial LE/\partial r_c$ are quite close; (3) when $r_c = 200$ (s/m), a unit increase of r_c would cause only 0.6 unit decrease on LE estimation.

We also plotted $\partial LE/\partial r_c$ as a function of r_c under different relative humidity conditions (RH varied from 30 to 90% with $R_n = 600$ W·m^{-2}, $U = 2$ m/s, and $T_a = 20$°C) in Figure 8(c). Similar to Figure 8(c), $\partial LE/\partial r_c$ with respect to r_c for different temperature (T_a varied from 5 to 40°C given $R_n = 600$ W·m^{-2}, $U = 2$ m/s, and RH = 0.6) are presented in Figure 8(d). Figures 8(c) and 8(d) also have similar patterns as Figure 8(a), and it can be seen that at $r_c = 200$ (s/m), $\partial LE/\partial r_c$ ranges from −0.77 to −0.53 in Figure 8(c) and ranges from −0.86 to −0.37 in Figure 8(d).

In summary, under a general moderate meteorological condition where $R_n = 600$ (W/m^2), $U = 2$ (m/s), RH = 0.6, and $T_a = 20$ (°C), if r_c is larger than 200 (s/m), $\partial LE/\partial r_c$ is less than 0.65; This implies that the predicted LE is not sensitive to the value of r_c used, when the average r_c is larger than 200. It is also important to note that Figures 8(a)–8(d) show that when r_c is small (<100 s/m), a unit increase of r_c could result in 1.34 units decrease on predicted LE. If this is the case of the site, then a variable r_c is needed. This provides an explanation for Lecina et al.'s [19] results where they found that a fixed canopy resistance (70 s/m) could provide good daily reference evapotranspiration estimation, but for the estimation of hourly reference evapotranspiration, variable canopy resistance values were needed; since their average

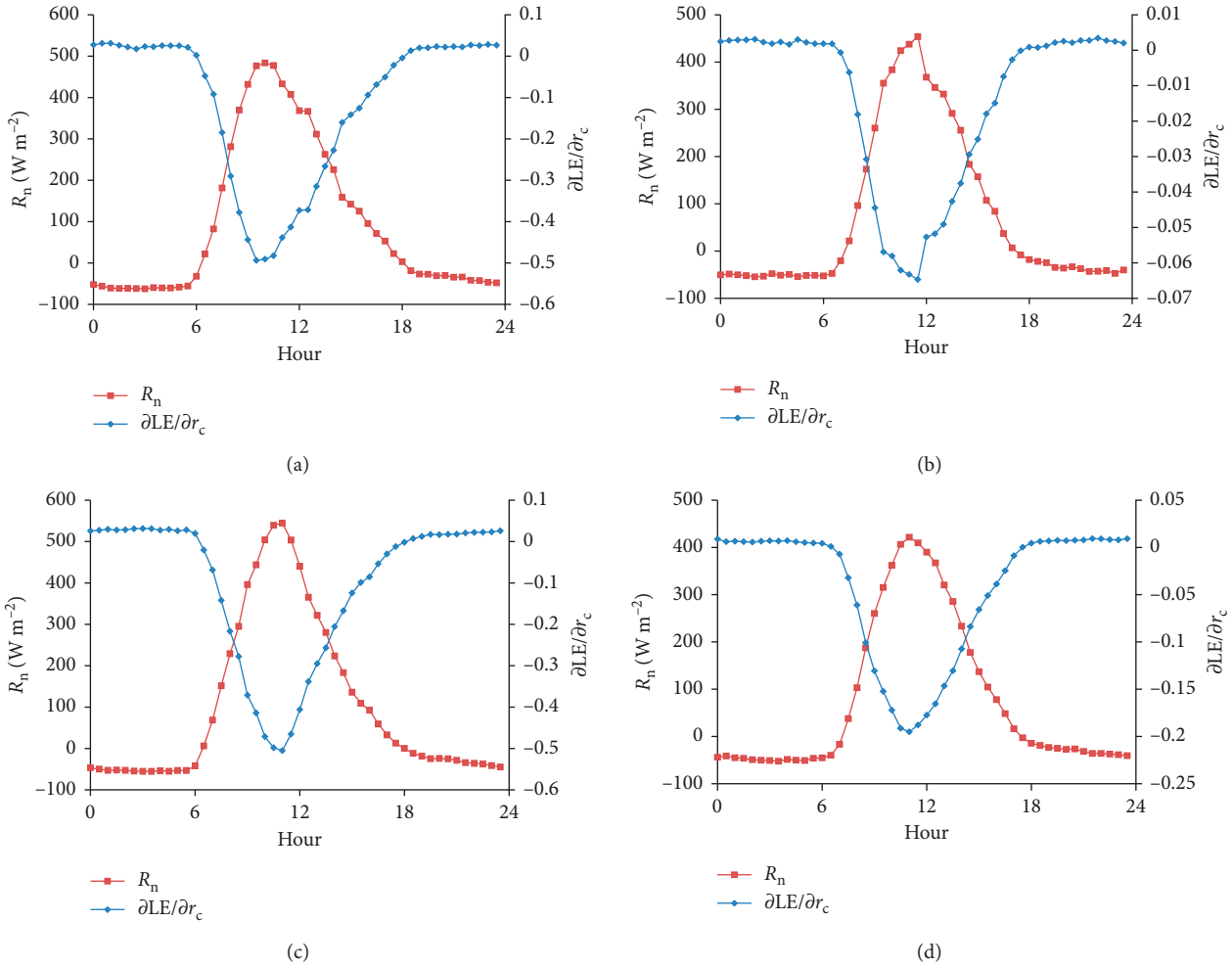

Figure 9: Diurnal variations of $\partial LE/\partial r_c$ and Rn for the season of (a) warm 2005, (b) cool 2005, (c) warm 2006, and (d) cool 2006.

canopy resistance was small (only 70 m/s). The values of $\partial LE/\partial r_c$ with respect to some certain r_c under $R_n = 600$ (W/m^2), RH = 0.6, $U = 2$ (m/s) at two different temperatures [$T_a = 20$ and 10 (°C)] are also listed in Table 3.

From Figures 8(a)–8(d), it is clear that under the conditions of low R_n, U, T_a, or vapor pressure deficit (i.e., high RH), the ratio of $\partial LE/\partial r_c$ is smaller. In other words, under a low wind speed, low temperature, small radiation, or low vapor pressure deficit condition, different r_c values will result in a relatively similar LE prediction. Hence, it does not matter much which r_c value is adopted. Also, from Table 3, it can be seen that when r_c is around 200 (s/m), a 100 units (s/m) increase of r_c only causes a 46–65 unit (W·m^{-2}) decrease on LE. These explained why a fixed constant r_c worked well for estimating diurnal LE while, in fact, r_c varied with time.

We also applied the measured data to equation (11). Figure 9 plots $\partial LE/\partial r_c$ as a function of time with measured R_n, T_a, U, and RH. In Figure 9, $\partial LE/\partial r_c$ varied in consistence with R_n; hence, at this site, R_n was the major (primary regulator) parameter controlling $\partial LE/\partial r_c$. The ratio of $\partial LE/\partial r_c$ was the lowest in the early morning and reached its maximum around 11:00, and then started to decrease in the afternoon. This diurnal trend is caused by the response of r_c to the increase of radiation, temperature, and other micrometeorological variables with time. Notice that the maximum values of $\partial LE/\partial r_c$ were only −0.5, −0.065, −0.5, and −0.2, respectively, for the warm and cool seasons of 2005 and 2006. This also indicated that a constant r_c was good enough for the whole diurnal LE estimation.

4.4. Energy Transfer Rate from Available Energy to LE. To explore the direct energy transfer rate (t_c) from available energy, Q_n, (here $Q_n \equiv R_n$) to LE, we plotted the diurnal pattern of averaged decoupling factor and energy transfer rate (equation (2)) in Figure 10. At the beginning of the morning, the decoupling coefficient was large due to the small value of r_c (Figure 5); and then following an increasing r_c, the decoupling coefficient then decreased to its lowest value around 10:00, then remained constant till around 14:00, and then increased again. In Figure 10, the direct energy transfer coefficient and the decoupling coefficient varied with the same pattern.

Also, it is noticed that on the basis of the linear relation between R_n and LE (shown in Figure 3) and equation (3), the

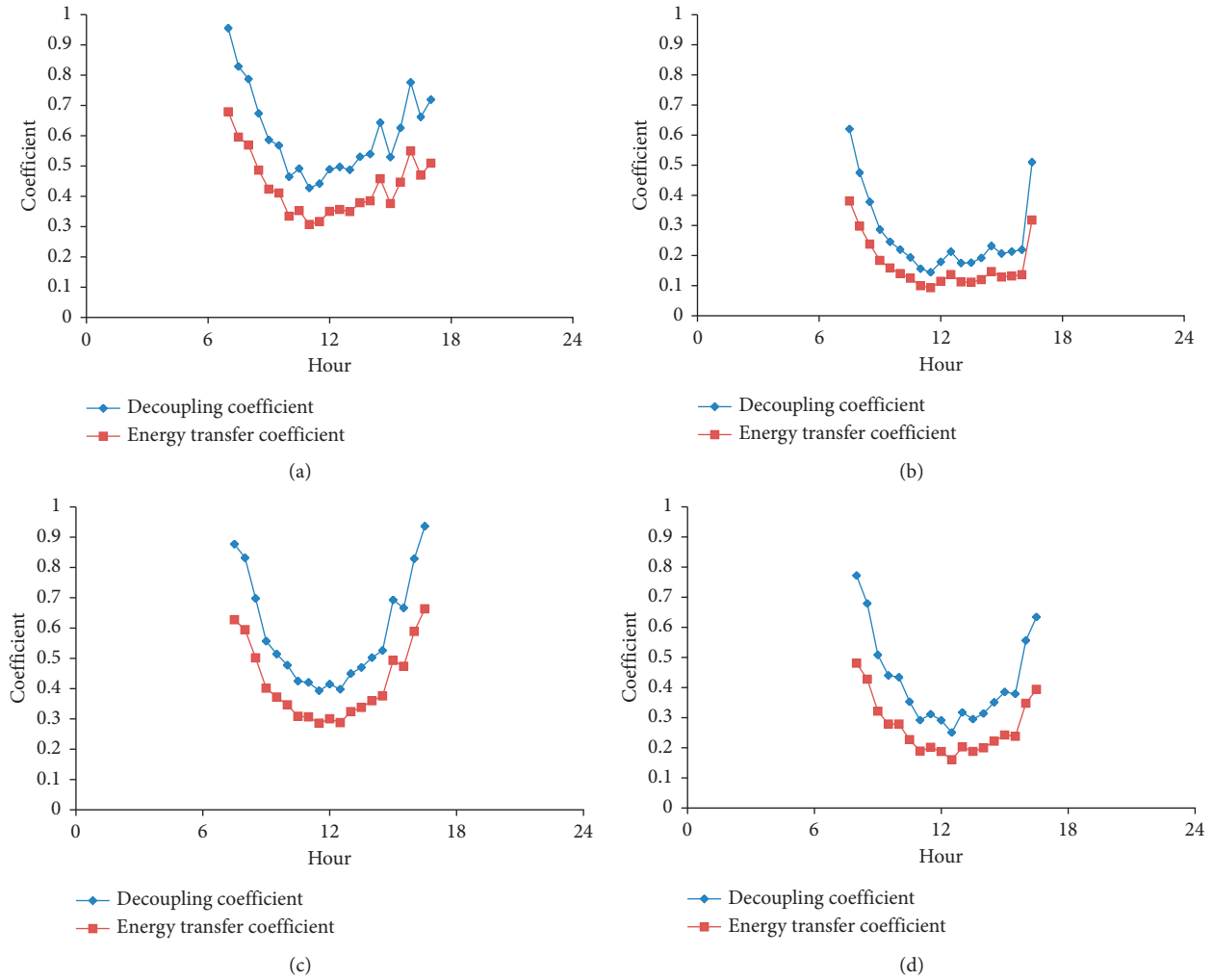

Figure 10: Diurnal variations of decoupling coefficient and energy transfer coefficient for the season of (a) warm 2005, (b) cool 2005, (c) warm 2006, and (d) cool 2006.

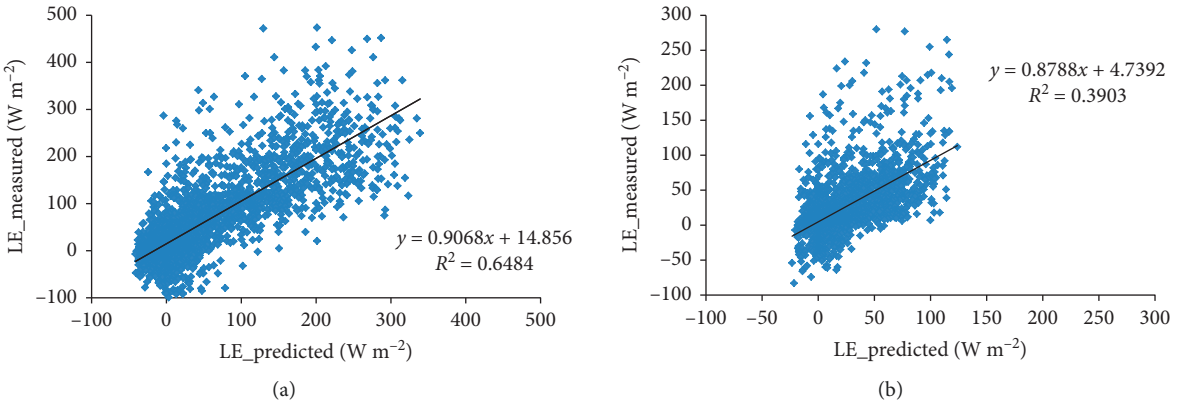

Figure 11: Continued.

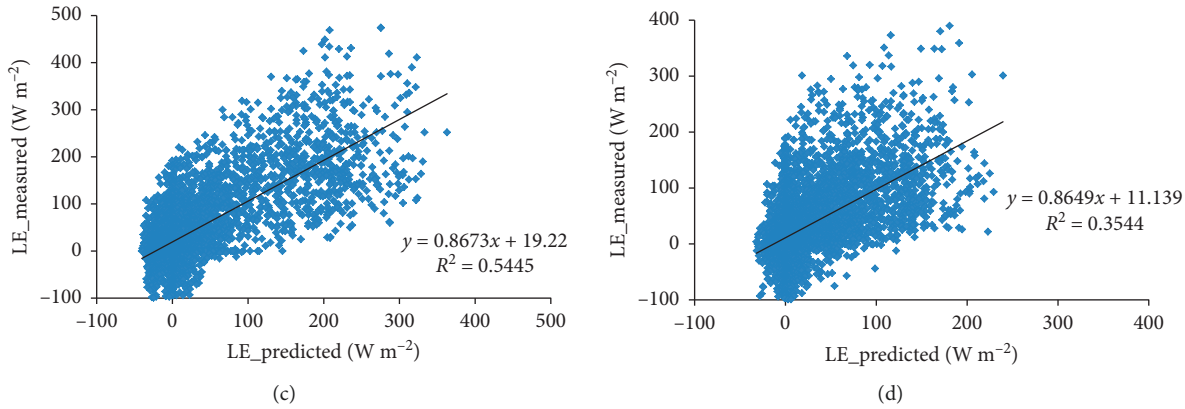

Figure 11: Comparisons between half-hourly measured and predicted LE (W·m^{-2}) for the season of (a) warm 2005, (b) cool 2005, (c) warm 2006, and (d) cool 2006.

slope of the regression between R_n and LE should be about the same as the averaged t_c in equation (3). We calculated the averaged t_c for the period of 10:00–14:00 when the canopy surface was dry. We found the averaged direct energy transfer rate for the warm and cool seasons of 2005 and 2006 were 0.35, 0.12, 0.32, and 0.20, respectively, and were about the same as the slope in that season shown in Figure 3 (these values were also listed in Table 1). Figure 10 and Table 1 demonstrated that the P–M equation was able to capture the energy transfer rate from Q_n to LE.

5. Conclusions

This study analyzed the two-year eddy-covariance flux measurements of sensible and latent heat above a humid montane Cypress forest in Taiwan and focused on the characteristics and estimation of evapotranspiration using the Penman–Monteith equation and the role of canopy resistance. Our results demonstrated the following:

(1) The evapotranspiration phenomenon controlled the micrometeorology on this site. In cool seasons, evapotranspiration was small and resulted in a higher percentage of net radiation distributing into sensible heat.

(2) Evapotranspiration above this site was mainly driven by the radiation energy and approached to the equilibrium status. And this is different from Jarvis and McNaughton [42] where they showed that forest generally has a smaller decoupling coefficient and the evapotranspiration rate is thus dominated by the atmospheric demand term.

(3) A fixed constant r_c is suitable for estimating the diurnal variation of ET for this site, but r_c should be varied with season. This also implies that the P–M equation is a good method for ET gap-filling if the canopy resistance is known a priori.

(4) When the average canopy resistance is higher than 200 (s/m), $\partial LE/\partial r_c$ is less than 0.65 under a general meteorological condition: $R_n = 600$ (W/m^2), $U = 2$ (m/s), $T_a = 20$ (°C), RH = 0.6; hence, a fixed canopy resistance is good enough for diurnal evapotranspiration estimation. However, when the average canopy resistance is less than 100 (s/m), $\partial LE/\partial r_c$ is bigger than 1.34 and variable canopy resistance are needed. These two constraints (200 and 100) were obtained based on purely analytical analyses and a measurement height around two times of the canopy height.

Appendix

Here we provide the comparisons between the half-hourly (not averaged) measured and predicted LE for each season in Figure 11. The constant canopy resistance adopted in each season was the same as listed in Table 2. It is not surprising that the agreements between the half-hourly measured and predicted LE were not as good as those for the seasonally averaged ones (Figure 4).

Data Availability

The data used to support the findings of this study are available from the corresponding author upon request.

Conflicts of Interest

The authors declare that they have no conflicts of interest.

Authors' Contributions

C.-I. H. conceived the research idea; B.-S. L. and C.-I. H. performed the model simulations; C.-I. H., B.-S. L., H. L., M.-C. H., and S. V. took part in the discussion, analysis, and interpretation of the data and model predictions; C.-I. H. and B.-S. L. wrote the manuscript. All authors reviewed the manuscript.

Acknowledgments

The data used for this study were from the project by YJ Hsia, SC Chang, and CI Hsieh under the contracts with Environmental Protection Agency, Taiwan (EPA-94-L105-02-

201 and EPA-96-FA11-03-A027-2). We are grateful to Miss Chih-Yi Fang who prepared the data for this study. This work was supported, in part, by the Ministry of Science and Technology, Taiwan (grant number: MOST-107-2410-H-002-172) and the Core Research Project, National Taiwan University (project numbers: NTU-CC-107L892606; NTU-CC-108L892606; NTU-CC-108L203313).

References

[1] Oak Ridge National Laboratory Distributed Active Archive Center (ORNL DAAC), *FLUXNET Web Page*, ORNL DAAC, Oak Ridge, TN, USA, 2015, http://fluxnet.ornl.gov.

[2] X. Bi, Z. Gao, X. Deng et al., "Seasonal and diurnal variations in moisture, heat, and CO_2 fluxes over grassland in the tropical monsoon region of southern China," *Journal of Geophysical Research: Atmospheres*, vol. 112, no. D10, 2007.

[3] D. Y. Hollinger, S. M. Goltz, E. A. Davidson, J. T. Lee, K. Tu, and H. T. Valentine, "Seasonal patterns and environmental control of carbon dioxide and water vapour exchange in an ecotonal boreal forest," *Global Change Biology*, vol. 5, no. 8, pp. 891–902, 1999.

[4] E. R. Humphreys, T. A. Black, G. J. Ethier et al., "Annual and seasonal variability of sensible and latent heat fluxes above a coastal Douglas-fir forest, British Columbia, Canada," *Agricultural and Forest Meteorology*, vol. 115, no. 1-2, pp. 109–125, 2003.

[5] G. Rana and N. Katerji, "Measurement and estimation of actual evapotranspiration in the field under Mediterranean climate: a review," *European Journal of Agronomy*, vol. 13, no. 2-3, pp. 125–153, 2000.

[6] R. G. Allen, L. S. Pereira, D. Raes, and M. Smith, *Crop Evapotranspiration —guidelines for Computing Crop Water Requirements: FAO Irrigation and Drainage Paper 56*, Food and Agriculture Organization, Rome, Italy, 1998.

[7] I. A. Walter, R. G. Allen, R. L. Elliott, D. Itenfisu, and P. Brown, "The ASCE standardized reference evapotranspiration equation," in *Standardization of Reference Evapotranspiration Task Committee Report*, ASCE Environmental and Water Resources Institute, Reston, VA, USA, 2001.

[8] J. B. Fisher, K. P. Tu, and D. D. Baldocchi, "Global estimates of the land-atmosphere water flux based on monthly AVHRR and ISLSCP-II data, validated at 16 FLUXNET sites," *Remote Sensing of Environment*, vol. 112, no. 3, pp. 901–919, 2008.

[9] A. Polhamus, J. B. Fisher, and K. P. Tu, "What controls the error structure in evapotranspiration models?," *Agricultural and Forest Meteorology*, vol. 169, pp. 12–24, 2013.

[10] J. Sheffield, E. F. Wood, and F. Munoz-Arriola, "Long-term regional estimates of evapotranspiration for Mexico based on downscaled ISCCP data," *Journal of Hydrometeorology*, vol. 11, no. 2, pp. 253–275, 2010.

[11] J. G. Alfieri, D. Niyogi, P. D. Blanken et al., "Estimation of the minimum canopy resistance for croplands and grasslands using data from the 2002 international H_2O project," *Monthly Weather Review*, vol. 136, no. 11, pp. 4452–4469, 2008.

[12] S. Irmak and D. Mutiibwa, "On the dynamics of canopy resistance: generalized linear estimation and relationships with primary micrometeorological variables," *Water Resources Research*, vol. 46, no. 8, 2010.

[13] P. G. Jarvis, "The interpretation of the variations in leaf water potential and stomatal conductance found in canopies in the field," *Philosophical Transactions of the Royal Society B: Biological Sciences*, vol. 273, no. 927, pp. 593–610, 1976.

[14] F. M. Kelliher, R. Leuning, M. R. Raupach, and E.-D. Schulze, "Maximum conductances for evaporation from global vegetation types," *Agricultural and Forest Meteorology*, vol. 73, no. 1-2, pp. 1–16, 1995.

[15] G. Zhang, G. Zhou, F. Chen, and Y. Wang, "Analysis of the variability of canopy resistance over a desert steppe site in inner Mongolia, China," *Advances in Atmospheric Sciences*, vol. 31, no. 3, pp. 681–692, 2014a.

[16] N. Katerji and G. Rana, "Modelling evapotranspiration of six irrigated crops under Mediterranean climate conditions," *Agricultural and Forest Meteorology*, vol. 138, no. 1–4, pp. 142–155, 2006.

[17] P. J. Perez, S. Lecina, F. Castellvi, A. Martínez-Cob, and F. J. Villalobos, "A simple parameterization of bulk canopy resistance from climatic variables for estimating hourly evapotranspiration," *Hydrological Processes*, vol. 20, no. 3, pp. 515–532, 2006.

[18] V. R. N. Pauwels and R. Samson, "Comparison of different methods to measure and model actual evapotranspiration rates for a wet sloping grassland," *Agricultural Water Management*, vol. 82, no. 1-2, pp. 1–24, 2006.

[19] S. Lecina, A. Martínez-Cob, P. J. Pérez, F. J. Villalobos, and J. J. Baselga, "Fixed versus variable bulk canopy resistance for reference evapotranspiration estimation using the Penman-Monteith equation under semiarid conditions," *Agricultural Water Management*, vol. 60, no. 3, pp. 181–198, 2003.

[20] Y. Kosugi, S. Takanashi, H. Tanaka et al., "Evapotranspiration over a Japanese cypress forest. I. Eddy covariance fluxes and surface conductance characteristics for 3 years," *Journal of Hydrology*, vol. 337, no. 3-4, pp. 269–283, 2007.

[21] C.-I. Hsieh, G. Kiely, A. Birkby, and G. Katul, "Photosynthetic responses of a humid grassland ecosystem to future climate perturbations," *Advances in Water Resources*, vol. 28, no. 9, pp. 910–916, 2005.

[22] G. Bala, K. Caldeira, M. Wickett et al., "Combined climate and carbon-cycle effects of large-scale deforestation," *Proceedings of the National Academy of Sciences*, vol. 104, no. 16, pp. 6550–6555, 2007.

[23] B. E. Law, E. Falge, L. Gu et al., "Environmental controls over carbon dioxide and water vapor exchange of terrestrial vegetation," *Agricultural and Forest Meteorology*, vol. 113, no. 1–4, pp. 97–120, 2002.

[24] K. Wang and R. E. Dickinson, "A review of global terrestrial evapotranspiration: observation, modeling, climatology, and climatic variability," *Reviews of Geophysics*, vol. 50, no. 2, 2012.

[25] L. A. Bruijnzeel, F. N. Scatena, and L. S. Hamilton, *Tropical Montane Cloud Forests: Science for Conservation and Management*, Cambridge University Press, Cambridge, UK, 2011.

[26] L. S. Hamilton, J. O. Juvik, and F. N. Scatena, "Tropical montane cloud forests," in *Ecological Studies*, vol. 110, p. 407, Springer-Verlag, New York, NY, USA, 1995.

[27] H. S. Chu, S. C. Chang, O. Klemm et al., "Does canopy wetness matter? Evapotranspiration from a subtropical montane cloud forest in Taiwan," *Hydrological Processes*, vol. 28, no. 3, 2012.

[28] F. Holwerda, L. A. Bruijnzeel, F. N. Scatena, H. F. Vugts, and A. G. C. A. Meesters, "Wet canopy evaporation from a Puerto Rican lower montane rain forest: the importance of realistically estimated aerodynamic conductance," *Journal of Hydrology*, vol. 414-415, pp. 1–15, 2012.

[29] C.-F. Li, D. Zelený, M. Chytrý et al., "Chamaecyparis montane cloud forest in Taiwan: ecology and vegetation classification," *Ecological Research*, vol. 30, no. 5, pp. 771–791, 2015.

[30] O. Klemm, S.-C. Chang, and Y.-J. Hsia, "Energy fluxes at a subtropical mountain cloud forest," *Forest Ecology and Management*, vol. 224, no. 1-2, pp. 5–10, 2006.

[31] I.-L. Lai, H. Scharr, A. Chavarria-Krauser et al., "Leaf growth dynamics of two congener gymnosperm tree species reflect the heterogeneity of light intensities given in their natural ecological niche," *Plant, Cell and Environment*, vol. 28, no. 12, pp. 1496–1505, 2005.

[32] I.-L. Lai, W. H. Schroeder, J.-T. Wu, L.-L. Kuo-Huang, C. Mohl, and C.-H. Chou, "Can fog contribute to the nutrition of *Chamaecyparis obtusa var. formosana*? Uptake of a fog solute tracer into foliage and transport to roots," *Tree Physiology*, vol. 27, no. 7, pp. 1001–1009, 2007.

[33] K. Mildenberger, E. Beiderwieden, Y.-J. Hsia, and O. Klemm, "CO_2 and water vapor fluxes above a subtropical mountain cloud forest-the effect of light conditions and fog," *Agricultural and Forest Meteorology*, vol. 149, no. 10, pp. 1730–1736, 2009.

[34] E. Beiderwieden, V. Wolff, Y.-J. Hsia, and O. Klemm, "It goes both ways: measurements of simultaneous evapotranspiration and fog droplet deposition at a montane cloud forest," *Hydrological Processes*, vol. 22, no. 21, pp. 4181–4189, 2008.

[35] S.-C. Chang, C.-F. Yeh, M.-J. Wu, Y.-J. Hsia, and J.-T. Wu, "Quantifying fog water deposition by in situ exposure experiments in a mountainous coniferous forest in Taiwan," *Forest Ecology and Management*, vol. 224, no. 1-2, pp. 11–18, 2006.

[36] M. Aubinet, A. Grelle, A. Ibrom et al., "Estimates of the annual net carbon and water exchange of forests: the EUROFLUX methodology," *Advances in Ecological Research*, vol. 30, pp. 113–175, 2000.

[37] C.-I. Hsieh, M.-C. Lai, Y.-J. Hsia, and T.-J. Chang, "Estimation of sensible heat, water vapor, and CO_2 fluxes using the flux-variance method," *International Journal of Biometeorology*, vol. 52, no. 6, pp. 521–533, 2008.

[38] C. J. Moore, "Frequency response corrections for eddy correlation systems," *Boundary-Layer Meteorology*, vol. 37, no. 1-2, pp. 17–35, 1986.

[39] J. M. Wilczak, S. P. Oncley, and S. A. Stage, "Sonic anemometer tilt correction algorithms," *Boundary-Layer Meteorology*, vol. 99, no. 1, pp. 127–150, 2001.

[40] E. K. Webb, G. I. Pearman, and R. Leuning, "Correction of flux measurements for density effects due to heat and water vapour transfer," *Quarterly Journal of the Royal Meteorological Society*, vol. 106, no. 447, pp. 85–100, 1980.

[41] K. G. McNaughton and P. G. Jarvis, "Predicting effects of vegetation changes on transpiration and evaporation," in *Water Deficit and Plant Growth*, T. T. Koslowski, Ed., vol. 7Academic Press, New York, NY, USA, pp. 1–47, 1983.

[42] P. G. Jarvis and K. G. McNaughton, "Stomatal control of transpiration: scaling up from leaf to region," *Advances in Ecological Research*, vol. 15, pp. 1–49, 1986.

[43] S. Li, L. Zhang, S. Kang et al., "Comparison of several surface resistance models for estimating crop evapotranspiration over the entire growing season in arid regions," *Agricultural and Forest Meteorology*, vol. 208, pp. 1–15, 2015.

[44] Q. Zhang, S. Manzoni, G. Katul, A. Porporato, and D. Yang, "The hysteretic evapotranspiration—vapor pressure deficit relation," *Journal of Geophysical Research: Biogeosciences*, vol. 119, no. 2, pp. 125–140, 2014.

[45] P. D. Blanken and T. A. Black, "The canopy conductance of a boreal aspen forest, Prince Albert National Park, Canada," *Hydrological Processes*, vol. 18, no. 9, pp. 1561–1578, 2004.

[46] W.-Z. Zhao, X.-B. Ji, E.-S. Kang, Z.-H. Zhang, and B.-W. Jin, "Evaluation of Penman-Monteith model applied to a maize field in the arid area of Northwest China," *Hydrology and Earth System Sciences*, vol. 14, no. 7, pp. 1353–1364, 2010.